

## An NMR Study on Dynamics of $AX_3$ Spin System as Illustrated By Methyl Group in 2,6-Dichlorotoluene

Jung-Rae Rho, Hyun Namgoong, and Jo Woong Lee\*

Department of Chemistry, and Institute of Molecular Science, College of Natural Sciences,  
Seoul National University, Seoul 151-742, Korea

Received June 13, 1998

The study of coupled relaxation for methyl spin system in 2,6-dichlorotoluene was performed on the basis of the magnetization mode formalism. Using five initial perturbing pulse sequences, eight experimental data sets were obtained, which were fitted with theoretical expressions with nine spectral density parameters. The same experiment was carried out at both 50.3 MHz and 125.6 MHz in carbon frequency. The measured spectral densities at both fields are similar in the exception of that related with carbon random field term. Furthermore, from the dipolar spectral density, the physical values may be extracted depending on the model of molecular reorientation. For example, it was assumed that the molecular framework undergoes asymmetric diffusive rotational process and methyl group reorients by either diffusive rotation about its symmetry axis or jump among internal rotational potential minima.

### Introduction

Methyl group, ubiquitous in the world of organic molecules, normally undergoes very anisotropic motions in liquid phase, because its rotation about the axis of symmetry is usually known to suffer very little frictions from neighboring solvent molecules, thus being described better in terms of the inertial (or free) rotational model, while rotation of the entire molecule on which it is embedded is often satisfactorily explained in the diffusional limit where the viscous drag forces from surrounding solvent molecules play a dominant role.<sup>1-3</sup> Consequently, fluctuation of the local magnetic fields at the site of a magnetic nucleus located on a methyl group can be anisotropic as well. That is, temporal correlations of the fluctuating local magnetic fields arising from dipolar interactions among magnetic nuclei of interest must be described by two or more correlation times differing substantially in magnitude. Furthermore, for nuclei on methyl group there can be another important source of fluctuating magnetic fields originating from spin-rotation interaction.<sup>4</sup> This interaction is known to be able to provide an effective relaxation pathway for the nuclei located on methyl group undergoing fast internal rotations and description of the nuclear magnetic relaxation due to this mechanism requires a few additional correlation times which differ in nature from those involved in dipolar mechanism.<sup>5</sup> All these conspire to make the interpretation of resulting nuclear magnetic relaxation data for the nuclei located on methyl group a difficult and messy job.

In principle, if all the necessary NMR relaxation data are at our disposal, we would be able to gain insight into detailed dynamics of methyl group by estimating the relevant correlation times (or the corresponding spectral densities). In reality, however, the amount of experimental data we can manage to obtain is often not quite sufficient to make this feasible. For example, measurement of the spin-lattice relaxation time  $T_1$  by the conventional inversion recovery method yields only one correlation time which is

hardly enough to provide us a glimpse into the details of complicated molecular dynamics.<sup>6</sup> Thus, it is quite natural to attempt to devise more sophisticated methods that can produce more revealing experimental data. Coupled relaxation experiment is one of those techniques designed specifically for this purpose where relaxations of  $^{13}\text{C}$  spins are observed with spin-spin couplings with protons being fully retained.<sup>7-9</sup>

In earlier days the proton relaxation study was the principal source of information about motional behaviors of methyl group.<sup>10</sup> The spin-lattice relaxation of methyl protons was intensively investigated theoretically by Hubbard,<sup>11</sup> Lynden-Bell,<sup>12</sup> and others<sup>13,14</sup> who treated these protons as an  $A_3$  spin system. They have concluded that relaxation of methyl protons involves several different magnetization modes each of which decays with its own characteristic decay constant and observation of their relaxation can provide us a few more useful dynamical parameters other than  $T_1$ . However, use of  $^{13}\text{C}$  as a probe nucleus turned out to enjoy more advantages than use of protons except for weaker signal intensities due to much lower natural abundance of the former, because in the case of  $^{13}\text{C}$  one may treat methyl spin system as an  $AX_3$  system for which more magnetization modes are available for observation.<sup>15</sup> Furthermore, by employing  $^{13}\text{C}$  as the probe nucleus, we may omit the laborious dilution procedure for eliminating the contributions from intermolecular dipole-dipole interactions as well.<sup>16</sup>

Theoretical foundation of treating methyl group as an  $AX_3$  spin system has already been laid by Grant *et al.*<sup>8,17</sup> but they have dealt only two leading relaxation mechanisms, dipolar and spin-rotation interactions. In the observation of the nuclei with electronically very anisotropic surroundings under very high magnetic fields a third relaxation mechanism known as the chemical shift anisotropy (CSA) often plays a crucial role, providing another useful information.<sup>18</sup> In our treatment of  $AX_3$  spin system we have slightly modified the formulation by Grant *et al.* following the procedure described by Canet<sup>9</sup> so that the contribution from the CSA may be explicitly included although this is not expected to be too important for methyl carbon-13. In this paper we have

\*To whom correspondence should be addressed

observed the relaxation of various <sup>13</sup>C magnetization modes for 2,6-dichlorotoluene dissolved in CDCl<sub>3</sub> and estimated the magnitude of various spectral densities involved on the basis of a few simple dynamics models, thereby elucidating the relative importance of various relaxation mechanisms operating for methyl carbon-13 as well as dynamical feature of methyl group itself.

### Theory of Relaxation of Magnetization Modes

The formulation of relaxation theory in the coupled system was described by the magnetization mode formalism introduced by Grant *et al.*,<sup>8,19</sup> who defined a magnetization mode as the trace over product of deviation density operator with a corresponding irreducible spherical tensor operator. All the magnetization modes possible for an AX<sub>3</sub> spin system are listed in Table 1, but among them only three antisymmetric modes plus two symmetric modes are quantities experimentally observable in liquid state, each of which can be expressed as a linear combination of intensities of methyl carbon-13 quartet and proton doublet lines, as shown follows:

$${}^a v_1 = \frac{1}{2} \text{Tr} [I_z^C \chi] = (1/k_C)(l_1 + l_2 + l_3 + l_4)$$

$${}^a v_2 = \frac{1}{2\sqrt{3}} \text{Tr} [(I_z^H + I_z^H + I_z^H) \chi] = (1/k_H)(l_5 + l_6)$$

**Table 1.** Magnetization Modes for the CH<sub>3</sub> Spin System

${}^a v_1 = \text{Tr} \{ \chi \frac{1}{2} I_z^C \}$
${}^a v_2 = \text{Tr} \{ \chi \frac{1}{2\sqrt{3}} (I_z^H + I_z^H + I_z^H) \}$
${}^a v_3 = \text{Tr} \{ \chi \frac{2}{\sqrt{3}} I_z^C (I_z^H I_z^H + I_z^H I_z^H + I_z^H I_z^H) \}$
${}^a v_4 = \text{Tr} \{ \chi 2 I_z^H I_z^H I_z^H \}$
${}^a v_5 = \text{Tr} \{ \chi \frac{2}{\sqrt{6}} [I_z^H (I_x^H I_x^H + I_y^H I_y^H) + I_z^H (I_x^H I_x^H + I_y^H I_y^H) + I_z^H (I_x^H I_x^H + I_y^H I_y^H)] \}$
${}^a v_6 = \text{Tr} \{ \chi \frac{2}{\sqrt{6}} [I_z^C (I_x^H I_x^H + I_y^H I_y^H) + I_x^H I_x^H + I_y^H I_y^H + I_x^H I_x^H + I_y^H I_y^H] \}$
${}^s v_7 = \text{Tr} \{ \chi \frac{1}{\sqrt{3}} I_z^C (I_z^H + I_z^H + I_z^H) \}$
${}^s v_8 = \text{Tr} \{ \chi 4 I_z^C I_z^H I_z^H I_z^H \}$
${}^s v_9 = \text{Tr} \{ \chi \frac{1}{\sqrt{3}} (I_z^H I_z^H + I_z^H I_z^H + I_z^H I_z^H) \}$
${}^s v_{10} = \text{Tr} \{ \chi \frac{1}{\sqrt{6}} (I_x^H I_x^H + I_y^H I_y^H + I_x^H I_x^H + I_y^H I_y^H + I_x^H I_x^H + I_y^H I_y^H) \}$
${}^s v_{11} = \text{Tr} \{ \chi \frac{2}{\sqrt{6}} [I_z^C I_z^H (I_x^H I_x^H + I_y^H I_y^H) + I_z^C I_z^H (I_x^H I_x^H + I_y^H I_y^H) + I_z^C I_z^H (I_x^H I_x^H + I_y^H I_y^H)] \}$
${}^s v_{12} = \text{Tr} \{ \chi E / 4 \}$

In expressions,  $\chi$  is the deviation density operator defined as  $\sigma - \sigma^T$ , where  $\sigma$  is spin operator and the superscript T denotes thermal equilibrium value.

$${}^a v_3 = \frac{2}{\sqrt{3}} \text{Tr} [I_z^C (I_z^H I_z^H + I_z^H I_z^H + I_z^H I_z^H) \chi]$$

$$= (1/k_C)(3l_1 - l_2 - l_3 + 3l_4)$$

$${}^s v_7 = \frac{1}{\sqrt{3}} \text{Tr} [I_z^C (I_z^H + I_z^H + I_z^H) \chi] + (1/k_C)(-3l_1 - l_2 + l_3 + 3l_4)$$

$${}^s v_8 = 4 \text{Tr} [I_z^C I_z^H I_z^H I_z^H \chi] = (1/k_C)(-l_1 + l_2 - l_3 + l_4) \quad (1)$$

where  $l_i$  ( $i=1, 2, 3, 4$ ) is the intensity of  $i$ th line in the carbon quartet and  $l_5$  and  $l_6$  are, respectively, those of proton doublet lines.  $k_C$  and  $k_H$  are proportional constants characteristic of carbon and proton signals, respectively. And superscripts in the upper left corner of notations for magnetization modes denote their parity with respect to the operation of spin inversion.

The dynamical evolution of the nuclear spin system can be described by the following equation:

$$\frac{d v_i(t)}{dt} = - \sum_j \Gamma_{ij} v_j(t) \quad (2)$$

where  $v_i(t)$  denotes the  $i$ th magnetization mode and  $\Gamma_{ij}$  represents the  $ij$ -element of the relaxation matrix which can be expressed as a linear combination spectral density terms.

Magnetization modes can be classified according to their symmetric or antisymmetric parity with respect to the operation of total spin inversion. This operation can be seen as exchanging all spin functions  $\alpha$  into  $\beta$  and *vice versa*. Any individual  $I_z$  operator is transformed into its opposite on this operation, which leaves Eq. 2 unchanged. But there arises a situation where  $\Gamma_{ij}$  transforms into  $-\Gamma_{ij}$  for two modes  $i$  and  $j$  of different parity. In that case, the only possible value for  $\Gamma_{ij}$  is zero. In other words, symmetric modes do not couple into antisymmetric modes and *vice versa*. This situation prevails in an isotropic medium and the only exception occurs when dipolar interaction couples with chemical shift anisotropy. In this exceptional case the coupling terms between symmetric and antisymmetric modes may be made to be nonvanishing through the cross-correlation mechanism between the dipolar interaction and chemical shift anisotropy. The expressions for  $\Gamma_{ij}$ 's for CH<sub>3</sub> spin system are summarized in Table 2 and the definitions and physical meanings for all the symbols and notations appearing in this table are given by Grant *et al.*<sup>8</sup> and also by Rho.<sup>20</sup> In general, the procedure of obtaining the formal expression for each  $\Gamma_{ij}$  is quite tedious and lengthy, albeit straightforward, and we will not duplicate it here since it has been described in detail elsewhere.<sup>9,20-21</sup>

It is straightforward to evaluate the dipolar spectral density data in the relaxation matrix if a model of molecular reorientational process is assumed. Conversely, various dynamics parameters relevant to an assumed model of reorientational process can be estimated if sufficient amount of dipolar spectral density data are available. In order to obtain some tangible results we assumed in this paper that the molecular framework undergoes asymmetric diffusive rotational motions while methyl group reorients by either diffusive rotation about its symmetry axis or jump among internal rotational potential minima. We further assumed that end-over-end rotation of molecular framework is independent of motions of methyl group. After a lengthy but straightforward discussion we can derive the following expression for the spectral densities between  $ij$  and  $kl$

**Table 2.** Expressions of Relaxation Matrix  $\Gamma_{ij}$  for the CH<sub>3</sub> Spin System

$$\begin{aligned}
{}^a \Gamma_{11} &= 10J_{\text{CH}} + 2j_{\text{C}}^{\text{RF}} & {}^a \Gamma_{12} &= \frac{5\sqrt{3}}{3} J_{\text{CH}} \\
{}^a \Gamma_{13} &= 2\sqrt{3}K_{\text{HCH}} & {}^a \Gamma_{14} &= {}^a \Gamma_{15} = 0 \\
{}^a \Gamma_{16} &= \frac{7\sqrt{6}}{3} K_{\text{HCH}} & {}^a \Gamma_{22} &= \frac{10}{3} J_{\text{CH}} + 10J_{\text{HH}} + 2j_{\text{H}}^{\text{RF}} \\
{}^a \Gamma_{23} &= 4K_{\text{CHH}} & {}^a \Gamma_{24} &= 2\sqrt{3}K_{\text{HHH}} & {}^a \Gamma_{25} &= 2\sqrt{2}K_{\text{HHH}} \\
{}^a \Gamma_{26} &= \sqrt{2}\left(\frac{5}{3}K_{\text{HCH}} - 2K_{\text{CHH}}\right) \\
{}^a \Gamma_{33} &= \frac{22}{3} J_{\text{CH}} + 12J_{\text{HH}} + 4K_{\text{HCH}} + 4K_{\text{HHH}} + 2j_{\text{C}}^{\text{RF}} + 4j_{\text{H}}^{\text{RF}} \\
{}^a \Gamma_{34} &= \sqrt{3}\left(4K_{\text{CHH}} + \frac{5}{3}J_{\text{CHH}}\right) \\
{}^a \Gamma_{35} &= -\sqrt{2}\left(2K_{\text{CHH}} + 2K_{\text{CHHH}} + \frac{5}{3}K_{\text{HCH}}\right) \\
{}^a \Gamma_{36} &= -\sqrt{2}\left(J_{\text{HH}} + K_{\text{HCH}} + 7K_{\text{HHH}} + 2k_{\text{HH}}\right) \\
{}^a \Gamma_{44} &= 10J_{\text{CH}} + 6J_{\text{HH}} + 6j_{\text{H}}^{\text{RF}} \\
{}^a \Gamma_{45} &= -\sqrt{6}\left(\frac{10}{3}K_{\text{HCH}} + J_{\text{HH}} + K_{\text{HHH}} + 2k_{\text{HH}}\right) \\
{}^a \Gamma_{46} &= -2\sqrt{6}K_{\text{CHHH}} \\
{}^a \Gamma_{55} &= 10J_{\text{CH}} + 7J_{\text{HH}} + \frac{10}{3}K_{\text{HCH}} + K_{\text{HCH}} + K_{\text{HHH}} + 6j_{\text{H}}^{\text{RF}} + 2k_{\text{HH}}^{\text{RF}} \\
{}^a \Gamma_{56} &+ \frac{5}{3}J_{\text{CH}} + 6K_{\text{CHH}} - 2K_{\text{CHHH}} + \frac{5}{3}K_{\text{HCH}} \\
{}^a \Gamma_{66} &= 8J_{\text{CH}} + 11J_{\text{HH}} - 3K_{\text{HHH}} + \frac{10}{3}K_{\text{HCH}} + 2j_{\text{C}}^{\text{RF}} + 4j_{\text{H}}^{\text{RF}} - 2k_{\text{HH}}^{\text{RF}} \\
{}^s \Gamma_{77} &= \frac{26}{3} J_{\text{CH}} + 10J_{\text{HH}} + 4K_{\text{HCH}} + 2j_{\text{C}}^{\text{RF}} + 2j_{\text{H}}^{\text{RF}} \\
{}^s \Gamma_{78} &= 2\sqrt{3}(K_{\text{HCH}} + K_{\text{HHH}}) & {}^s \Gamma_{79} &= \frac{10}{3} J_{\text{CH}} + 4K_{\text{CHH}} \\
{}^s \Gamma_{710} &= -\sqrt{2}\left(\frac{5}{3}K_{\text{HCH}} + 2K_{\text{CHH}}\right) & {}^s \Gamma_{711} &= \sqrt{2}\left(\frac{7}{3}K_{\text{HCH}} + 2K_{\text{HHH}}\right) \\
{}^s \Gamma_{88} &= 6J_{\text{CH}} + 6J_{\text{HH}} + 2j_{\text{C}}^{\text{RF}} + 6j_{\text{H}}^{\text{RF}} \\
{}^s \Gamma_{89} &= 4\sqrt{3}K_{\text{CHH}} & {}^s \Gamma_{810} &= 2\sqrt{6}K_{\text{CHHH}} \\
{}^s \Gamma_{811} &= -\sqrt{6}\left(J_{\text{HH}} + K_{\text{HCH}} + K_{\text{HHH}} + 2k_{\text{HH}}^{\text{RF}}\right) \\
{}^s \Gamma_{88} &= \frac{20}{3} J_{\text{CH}} + 12J_{\text{HH}} + 4K_{\text{HHH}} + 4j_{\text{H}}^{\text{RF}} \\
{}^s \Gamma_{910} &= -\sqrt{2}\left(J_{\text{HH}} + \frac{10}{3}K_{\text{HCH}} + 7K_{\text{HHH}} + 2k_{\text{HH}}^{\text{RF}}\right) \\
{}^s \Gamma_{911} &= -\sqrt{2}\left(2K_{\text{CHH}} + 2K_{\text{CHHH}} - \frac{5}{3}K_{\text{HCH}}\right) \\
{}^s \Gamma_{1010} &= \frac{20}{3} J_{\text{CH}} + 11J_{\text{HH}} - 3J_{\text{HHH}} - \frac{10}{3}K_{\text{HCH}} + 4j_{\text{H}}^{\text{RF}} - 2k_{\text{HH}}^{\text{RF}} \\
{}^s \Gamma_{1011} &= 6K_{\text{CHH}} - \frac{5}{3}K_{\text{HCH}} - 2K_{\text{CHHH}} \\
{}^s \Gamma_{1111} &= \frac{20}{3} J_{\text{CH}} + 7J_{\text{HH}} + K_{\text{HHH}} + \frac{2}{3}K_{\text{HCH}} + 2j_{\text{C}}^{\text{RF}} + 6j_{\text{H}}^{\text{RF}} + 2k_{\text{HH}}^{\text{RF}}
\end{aligned}$$

Notations of cross-correlation dipolar spectral density are simplified as follows:  $J_{\text{CHH}}^{\text{D}} = K_{\text{CHH}}$ ,  $J_{\text{CHHH}}^{\text{D}} = K_{\text{CHH}}$ ,  $J_{\text{HHHH}}^{\text{D}} = K_{\text{HHH}}$ ,  $J_{\text{CHHH}}^{\text{D}} = K_{\text{CHHH}}$

dipolar vectors:

$$J_{ij}^{\text{D}} = \frac{3}{40} \left( \frac{\gamma_i \gamma_j \gamma_k \gamma_l \hbar^2}{r_{ij}^3 r_{kl}^3} \right) \tau_{\text{D}} \quad (3)$$

where, assuming the axis of internal rotation coincides with

one of the three principal axes of overall rotational diffusion tensor, say the z-axis, the correlation time  $\tau_{\text{D}}$  is given by

$$\begin{aligned}
\tau_{\text{D}} &= \frac{c_1}{E_1 + 1/\tau_{\text{int}}^{(1)}} + \frac{c_1}{E_2 + 1/\tau_{\text{int}}^{(1)}} + \frac{c_2}{E_3 + 1/\tau_{\text{int}}^{(2)}} \\
&+ \frac{c_3}{E_4 + 1/\tau_{\text{int}}^{(2)}} + \frac{c_4}{E_5 + 1/\tau_{\text{int}}^{(2)}} + \frac{c_3}{E_4} + \frac{c_4}{E_5} \quad (4)
\end{aligned}$$

$E_1$  through  $E_5$  appearing in Eq. 4 are expressed in terms of the three principal values of rotational diffusion tensor,  $D_{xx}$ ,  $D_{yy}$ , and  $D_{zz}$  as follows:

$$\begin{aligned}
E_1 &= 4D_{xx} + D_{yy} + D_{zz} \\
E_2 &= D_{xx} + 4D_{yy} + D_{zz} \\
E_3 &= D_{xx} + D_{yy} + 4D_{zz} \\
E_4 &= 6D + 6\sqrt{D^2 - I^2} \\
E_5 &= 6D - 6\sqrt{D^2 - I^2} \quad (5)
\end{aligned}$$

with

$$\begin{aligned}
D &= (D_{xx} + D_{yy} + D_{zz})/3 \\
I^2 &= (D_{xx}D_{yy} + D_{yy}D_{zz} + D_{zz}D_{xx})/3 \quad (6)
\end{aligned}$$

And two correlation times relevant to internal rotation are defined as

$$\exp(-t/\tau_{\text{int}}^{(1)}) = \langle \exp[-i\phi(0)] \exp[i\phi(t)] \rangle \quad (7)$$

and

$$\exp(-t/\tau_{\text{int}}^{(2)}) = \langle \exp[-2i\phi(0)] \exp[2i\phi(t)] \rangle \quad (8)$$

where  $\phi(t)$  is the azimuthal angle that describes internal reorientation of methyl group. The coefficients  $c_i$ 's appearing in Eq. 4 depend on the orientations of two dipolar vectors  $ij$  and  $kl$  as follows:

$$\begin{aligned}
c_1 &= 6 \cos\theta_{ij} \cos\theta_{kl} \sin\theta_{ij} \sin\theta_{kl} \cos(\phi_{ij} - \phi_{kl}) \\
c_2 &= (3/2) \sin^2\theta_{ij} \sin^2\theta_{kl} \cos[2(\phi_{ij} - \phi_{kl})] \\
c_3 &= (3/2) \cos^2(\beta/2) \sin^2\theta_{ij} \sin^2\theta_{kl} \cos[2(\phi_{ij} - \phi_{kl})] \\
c_3 &= \sin^2(\beta/2) (3\cos^2\theta_{ij} - 1)(3\cos^2\theta_{kl} - 1) \\
c_4 &= (3/2) \sin^2(\beta/2) \sin^2\theta_{ij} \sin^2\theta_{kl} \cos[2(\phi_{ij} - \phi_{kl})] \\
c_4 &= \cos^2(\beta/2) (3\cos^2\theta_{ij} - 1)(3\cos^2\theta_{kl} - 1) \quad (9)
\end{aligned}$$

where  $\theta_{ij}$ ,  $\theta_{kl}$ ,  $\phi_{ij}$ , and  $\phi_{kl}$  denote the polar and azimuthal angles of dipolar vectors  $ij$  and  $kl$ , respectively, defined in the coordinates system shown in Figure 1 and the angle  $\beta$  is defined by

$$\beta = \tan^{-1}[\sqrt{3}(D_{xx} - D_{yy})/\{2D_{zz} - (D_{xx} + D_{yy})\}] \quad (10)$$

The two internal reorientational correlation times  $\tau_{\text{int}}^{(1)}$  and  $\tau_{\text{int}}^{(2)}$  can have various expressions depending on the assumed model for internal reorientation of methyl group. For example, if this reorientation takes place *via* diffusional steps, we find

$$\tau_{\text{int}}^{(1)} = 1/D_i \text{ and } \tau_{\text{int}}^{(2)} = 1/4D_i; \text{ that is } \tau_{\text{int}}^{(1)}/\tau_{\text{int}}^{(2)} = 4, \quad (11)$$

where  $D_i$  denotes the diffusion constant for reorientation of methyl group about its symmetry axis. On the other hand, the internal reorientation may proceed through jump by 120° or 60° among potential minima. For jump among potential minima, the ratio of  $\tau_{\text{int}}^{(1)}$  vs  $\tau_{\text{int}}^{(2)}$  varies over a certain range (possibly 1 to 3) depending on jump patterns. If the orientation takes place by 120° jumps among three equal

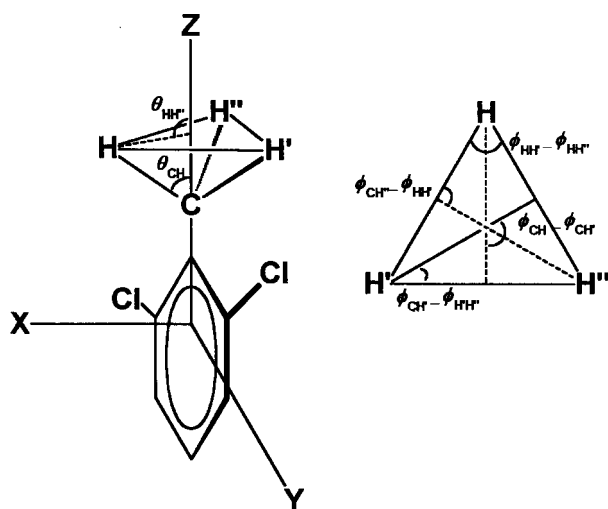


**Figure 1.** The coordinates of molecule and polar and azimuthal angles of dipolar vectors in CH<sub>3</sub>.

potential minima, we have

$$\tau_{int}^{(1)} = \tau_{int}^{(2)} = \tau_e/3; \text{ that is, } \tau_{int}^{(1)}/\tau_{int}^{(2)} = 1, \quad (12)$$

where  $1/\tau_e$  represents the jump rate from one site to another. We can also assume that the reorientation proceeds through jumps between only nearest sites among the 6-equivalent sites. In this case we can show that (see Appendix)

$$\tau_{int}^{(1)} = \tau_e \text{ and } \tau_{int}^{(2)} = \tau_e/3; \text{ that is } \tau_{int}^{(1)}/\tau_{int}^{(2)} = 3, \quad (13)$$

Yet, in another probable model these jumps may be assumed to take place between not only the nearest sites but also those further apart. In particular, if we take into consideration additional jumps between next-to-nearest sites, we have

$$\tau_{int}^{(1)} = \tau_e/4 \text{ and } \tau_{int}^{(2)} = \tau_e/6; \text{ that is } \tau_{int}^{(1)}/\tau_{int}^{(2)} = 3/2, \quad (14)$$

where we have assumed jumps among next-to-nearest sites occur with the same rate as those occurring between nearest sites (See, also, Appendix). Thus, to some extent one may use this ratio to justify the suitability of an adopted model to describe internal rotation of a methyl group.

## Experimentals and Calculations

### Experimentals

**Sample Preparation.** For our coupled relaxation study of CH<sub>3</sub> spin system, 2,6-dichlorotoluene (99%, not <sup>13</sup>C-enriched) and CDCl<sub>3</sub> (100%) were purchased from Aldrich Chemical Company and used without further purification. Twenty-five milligrams of 2,6-dichlorotoluene were dissolved in two milliliters of CDCl<sub>3</sub> to make a sample solution. After being placed in a 5 mm o.d. NMR tube, this sample was degassed by repeating the standard freeze-pump-thaw cycle at least five times and then sealed under vacuum.

**NMR Experiments.** NMR relaxation experiments were run on both Varian VXR200S and UNITY500 spectrometers. In VXR200S the <sup>13</sup>C frequency was 50.3 MHz and the <sup>1</sup>H frequency 200 MHz while in UNITY500 they were 125.6 MHz and 500 MHz, respectively. In our experiments only the <sup>13</sup>C signals were observed, for which the sample dilution

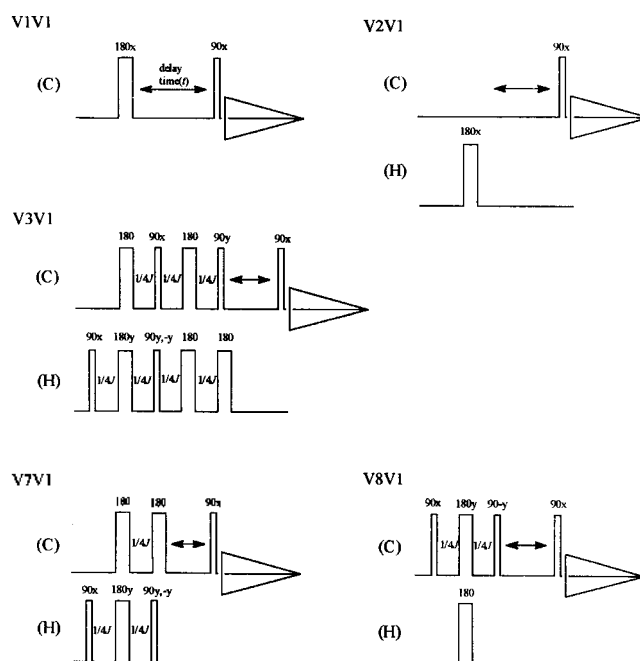


**Figure 2.** The pulse sequences used to obtain initial excitation of observable magnetization modes in the liquid state.

process may be omitted, thus saving a great deal of time and labor. Temperature was maintained at  $25 \pm 1$  °C throughout the experiments.

For coupled spin relaxation measurement five different types of initial spin states were prepared by applying the following five pulse sequences (see Figure 2):

- total carbon inversion (carbon hard pulse) - V1V1 pulse sequence
- total proton inversion (proton hard pulse) - V2V1 pulse sequence
- $\nu_3$  mode preparation - V3V1 pulse sequence
- $\nu_7$  mode preparation - V7V1 pulse sequence
- $\nu_8$  mode preparation - V8V1 pulse sequence

All the pulse sequences except V1V1 are not routinely available in the form of commercial pulse programs. So they were programmed and written in our laboratory with the MAGICAL Programming Language provided by the Varian Associates.<sup>22</sup> In the UNITY500 spectrometer, the normal  $\pi/2$  pulse lengths were, respectively, 12.5  $\mu$ sec for <sup>13</sup>C and 11.5  $\mu$ sec for <sup>1</sup>H while in the VXR200S they were 20  $\mu$ sec for <sup>13</sup>C and 22.5  $\mu$ sec for <sup>1</sup>H. The recycle time was set 10 times the  $T_1$  of methyl carbon and the FID observation was made for 17 different delay times,  $\tau$ . In the V1V1 and V8V1 sequence, twenty-four scans were accumulated for each given value of delay time,  $\tau$ , to achieve the required signal to noise ratio. However, in the other sequences the number of scans accumulated was reduced to eight due to the effect of possible polarization transfer from <sup>1</sup>H to <sup>13</sup>C. For observation of methyl carbon, a spectral width of 4000 Hz was used and 10 K data points were collected. Peak heights in the multiplet spectra were used to represent the magnetization mode intensities and each data presented in this paper represents the average of five independent measurements.

Since protons were not observed directly, <sup>1</sup>H  $\pi$  pulse

angles were adjusted by watching their effects on the spin echo of the coupled  $^{13}\text{C}$  doublet from the methine group.

### Calculations

Evolution of each magnetization mode can be pursued by solving the coupled differential equations given by Eq. 2. To facilitate this procedure we now introduce the "so-called" normal mode of magnetization,  $u_i$ , defined by

$$v_j = \sum_i Q_{ji} u_i \quad (15)$$

or,

$$v = Q \cdot u, \quad (16)$$

where  $Q$  is a transformation matrix that diagonalizes the relaxation matrix  $\Gamma$ .

Then, Eq. 2 may be rewritten in terms of the normal modes of magnetization as

$$\frac{d}{dt} u(t) = -\Lambda u(t) \quad (17)$$

where the diagonal matrix  $\Lambda$  is defined as

$$\Lambda = Q^{-1} \Gamma Q. \quad (18)$$

Eq. 17 tells us that each normal mode of magnetization  $u_i(t)$  evolves according to

$$\begin{aligned} u(t) &= \exp(-\Lambda t) u(0) \\ &= \exp(-Q^{-1} \Gamma Q t) u(0) \end{aligned} \quad (19)$$

Experimentally observed, however, are  $v_i(t)$ 's, not  $u_i(t)$ 's. Therefore, we substitute Eq. 19 back into Eq. 16 to obtain

$$v(t) = Q \exp(-Q^{-1} \Gamma Q t) Q^{-1} v(0) \quad (20)$$

Each coupled  $^{13}\text{C}$  spectra from the five different pulse sequence experiments for the methyl group gives the values of corresponding observable magnetization modes from the linear combination of four lines as presented in the Eq. 1. These quantities may also be expressed in terms of the elements of  $Q$  and the eigenvalues of  $\Gamma$  in the Eq. 20 as follows:

#### a) V1V1 pulse sequence experiment

$$\begin{aligned} y_1(t) &= {}^a v_1(t) / \langle I_z^F(eq) \rangle = -2 \sum_{i=1}^{11} Q_{1i} Q_{1i} \exp(-\lambda_i t) \\ y_2(t) &= {}^a v_3(t) / \langle I_z^F(eq) \rangle = -2\sqrt{3} \sum_{i=1}^{11} Q_{3i} Q_{1i} \exp(-\lambda_i t) \end{aligned} \quad (21)$$

#### b) V2V1 pulse sequence experiment

$$\begin{aligned} y_3(t) &= {}^a v_1(t) / \langle I_z^F(eq) \rangle = -2\sqrt{3} (\gamma_H / \gamma_C) \sum_{i=1}^{11} Q_{1i} Q_{2i} \exp(-\lambda_i t) \\ y_4(t) &= {}^a v_3(t) / \langle I_z^F(eq) \rangle = -6 (\gamma_H / \gamma_C) \sum_{i=1}^{11} Q_{3i} Q_{2i} \exp(-\lambda_i t) \end{aligned} \quad (22)$$

#### c) V3V1 pulse sequence experiment

$$y_5(t) = {}^a v_3(t) / {}^a v_3(0) = \sum_{i=1}^{11} Q_{3i} Q_{3i} \exp(-\lambda_i t) \quad (23)$$

#### d) V4V1 pulse sequence experiment

$$y_6(t) = {}^s v_7(t) / {}^s v_7(0) = \sum_{i=1}^{11} Q_{7i} Q_{7i} \exp(-\lambda_i t)$$

$$y_7(t) = {}^s v_8(t) / {}^s v_8(0) = 1/3 \sum_{i=1}^{11} Q_{8i} Q_{7i} \exp(-\lambda_i t) \quad (24)$$

#### e) V5V1 pulse sequence experiment

$$y_8(t) = {}^s v_8(t) / {}^s v_8(0) = \sum_{i=1}^{11} Q_{8i} Q_{8i} \exp(-\lambda_i t) \quad (25)$$

These eight quantities will depend nonlinearly upon nine unknown spectral density parameters involved in the  $Q$  and  $\lambda$ . A standard way to extract these parameters from the observed data is to seek the best set of parameter values that minimizes the merit function  $S^2$  defined by

$$S^2 = \sum_{k=1}^8 \sum_{i=1}^{17} [e_k(t_i, \text{exp}) - y_k(t_i)]^2, \quad (26)$$

where  $e_k(t_i, \text{exp})$  is the observed value of  $k$ th magnetization mode at time  $t_i$ , while  $y_k(t_i)$  is the value of the same magnetization mode at time  $t_i$ , calculated from Eqs. 21 through 25 for an arbitrarily set of parameter values.

With nonlinear dependencies the minimization process must proceed iteratively. For a given initial set of parameter values, a procedure is developed to improve the trial solutions. The procedure is then repeated until  $S^2$  no longer decreases. The Marquardt method<sup>23,24</sup> for fitting routine was adopted in this study. All of the theoretical equations were fitted simultaneously with experimental data with nine spectral densities.

## Results and Discussion

Relaxation data for all the possible magnetization modes in  $\text{CH}_3$  spin system generated by five different pulse sequences were plotted against delay times in Figures 3 through 5. The solid lines represent the results obtained by simultaneous least-squares fitting of all experimental data at a given field. The dipolar and random field spectral densities

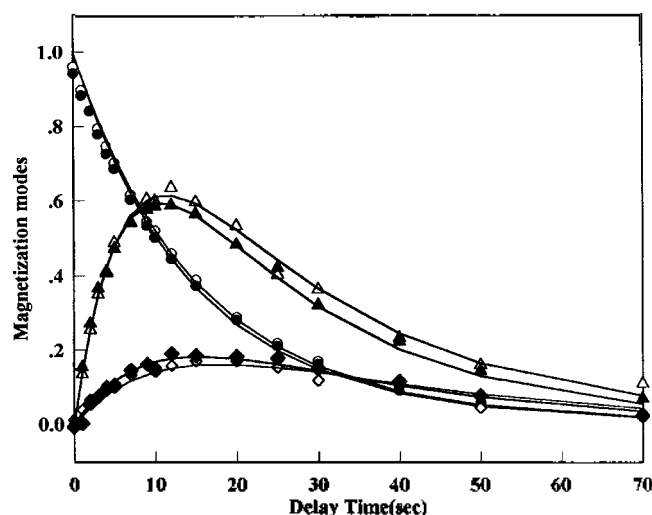


**Figure 3.** Plot of magnetization modes obtained from corresponding coupled spectra. The empty and filled symbols denote experimental data obtained at 50.3 MHz and 125.6 MHz, respectively and solid lines fitted curves.  $\circ$ :  $y_1$  (50.3 MHz),  $\bullet$ :  $y_1$  (125.6 MHz),  $\diamond$ :  $y_2$  (50.3 MHz),  $\blacklozenge$ :  $y_2$  (125.6 MHz),  $\triangle$ :  $y_3$  (50.3 MHz),  $\blacktriangle$ :  $y_3$  (125.6 MHz)

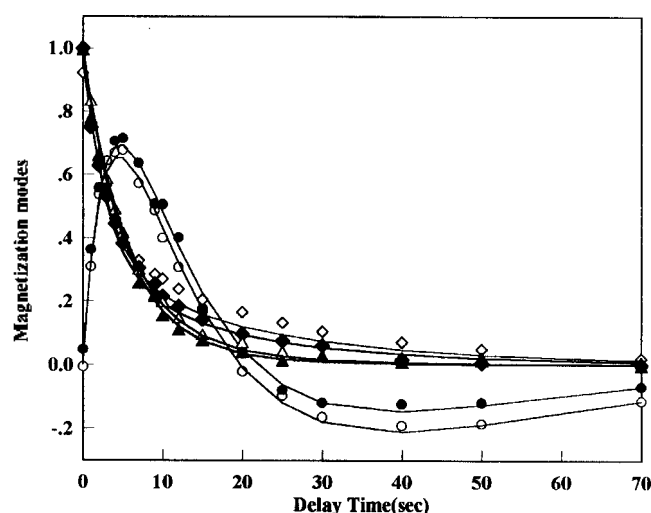


**Figure 4.** Plot of magnetization modes obtained from corresponding coupled spectra. The empty and filled symbols denote experimental data obtained at 50.3 MHz and 125.6 MHz, respectively and solid lines fitted curves.  $\circ$ :  $y_4$  (50.3 MHz),  $\bullet$ :  $y_4$  (125.6 MHz),  $\diamond$ :  $y_5$  (50.3 MHz),  $\blacklozenge$ :  $y_5$  (125.6 MHz),  $\triangle$ :  $y_6$  (50.3 MHz),  $\blacktriangle$ :  $y_6$  (125.6 MHz)

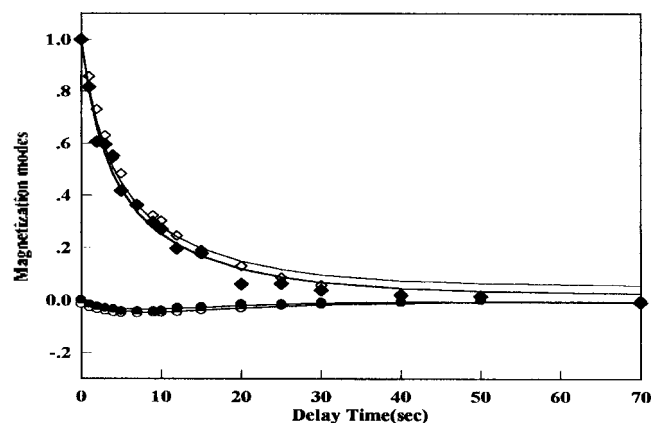


**Figure 5.** Plot of magnetization modes obtained from corresponding coupled spectra. 50.3 MHz and 125.6 MHz, respectively and solid lines fitted curves.  $\circ$ :  $y_7$  (50.3 MHz),  $\bullet$ :  $y_7$  (125.6 MHz),  $\diamond$ :  $y_8$  (50.3 MHz),  $\blacklozenge$ :  $y_8$  (125.6 MHz)

obtained by these fittings at two different magnetic fields are listed in Table 3, which shows that obtained spectral densities, except the carbon random field term  $j_C$ , depend very little on the field strength within experimental error. The slight dependency of  $j_C$  on the magnetic field strength suggests that at higher fields the chemical shift anisotropy may make some contribution, albeit small and unimportant, in the relaxation of methyl carbon-13 in 2,6-dichlorotoluene. This suggestion is also supported by the difference in the observed NOE's for the methyl spin system at two different magnetic fields as shown in Table 4. We could also evaluate the NOE's by making use of the spectral densities estimated from the foregone measurements through the following relation;<sup>25</sup>

$$\text{NOE} = 1 + \frac{\gamma_H}{\gamma_C} \frac{15J_{CH} - 200K_{HCH}^2}{30J_{CH} + 6j_C - 400K_{HCH}^2} \quad (27)$$

**Table 3.** Spectral Densities for Methyl System at Two Magnetic Fields

	50MHz	125MHz
$J_{CH}$	$0.0039 \pm 0.00005$	$0.0039 \pm 0.00006$
$K_{HCH}$	$0.0020 \pm 0.00011$	$0.0028 \pm 0.00014$
$K_{CHH}$	$0.0042 \pm 0.00010$	$0.0042 \pm 0.00009$
$K_{CHHH}$	$0.0022 \pm 0.00042$	$0.0020 \pm 0.00048$
$J_{HH}$	$0.0067 \pm 0.00025$	$0.0063 \pm 0.00024$
$K_{HHH}$	$0.0053 \pm 0.00025$	$0.0051 \pm 0.00027$
$j_C$	$0.0135 \pm 0.00069$	$0.0165 \pm 0.00075$
$j_H$	$0.0215 \pm 0.00095$	$0.0227 \pm 0.00094$
$k_{HH}$	$0.0269 \pm 0.00143$	$0.0253 \pm 0.00151$

**Table 4.** Comparison of Measured and Calculated NOE for CH<sub>3</sub> system

	50MHz	125MHz
Measured	2.274	2.023
Calculated	2.190	2.070

Calculated NOE was found to be in good agreement with measured one as shown in Table 4. The relaxation data for *para* methine <sup>13</sup>C may be similarly treated to obtain the various autocorrelation and dipolar-CSA cross-correlation spectral densities which are shown in Table 5. Unlike the case of methine carbon,  $j_C$  for methyl carbon is found to be of considerable magnitude due to the large contribution from the spin-rotational mechanism. From the dipolar spectral densities for methyl carbon three diffusion constants  $D_{xx}$ ,  $D_{yy}$ ,  $D_{zz}$  and two internal correlation times  $\tau_{int}^{(1)}$ ,  $\tau_{int}^{(2)}$  were uniquely determined<sup>26</sup> and are listed in the Table 6. The determined three diffusion constants were in turn used to evaluate the dipolar spectral density for *para*-methine carbon  $J_{CH}$  which agrees fairly well with the observed one as

**Table 5.** Spectral Densities for *para*-CH System in 2,6-dichlorotoluene

	50MHz	125MHz
$J_{CH}$	$0.0366 \pm 0.0003$	$0.0363 \pm 0.0006$
$J_{CSA}$	$0.0029 \pm 0.0004$	$0.0114 \pm 0.0007$
$K_{C-CSA}$	$-0.0048 \pm 0.0002$	$-0.0114 \pm 0.0005$
$j_H$	$0.0232 \pm 0.0001$	$0.0264 \pm 0.0020$
$K_{H-CSA}$	$-0.0003 \pm 0.00007$	$-0.0008 \pm 0.00002$

**Table 6.** Diffusion Constants and Internal Correlation Times

	50MHz	125MHz
$D_{xx}$ ( $10^{10} \text{s}^{-1}$ )	$4.17 \pm 0.15$	$4.28 \pm 0.12$
$D_{yy}$ ( $10^{10} \text{s}^{-1}$ )	$4.08 \pm 0.10$	$4.12 \pm 0.07$
$D_{zz}$ ( $10^{10} \text{s}^{-1}$ )	$4.03 \pm 0.11$	$4.10 \pm 0.11$
$1/\tau_{int}^{(1)}$ ( $10^{12} \text{s}^{-1}$ )	$2.41 \pm 0.17$	$2.63 \pm 0.09$
$1/\tau_{int}^{(2)}$ ( $10^{12} \text{s}^{-1}$ )	$4.18 \pm 0.25$	$4.61 \pm 0.12$
$\tau_{int}^{(1)}/\tau_{int}^{(2)}$	1.73	1.75

**Table 7.** Spectral Density ( $J_{CH}$ ) in *para*-CH Determined from Diffusion Constants Listed in Table 6 in Comparison with Observed Value

	50MHz	125MHz
$J_{CH}$ (Measured)	$0.0366 \pm 0.0003$	$0.0363 \pm 0.0006$
$J_{CH}$ (Calculated)	$0.0285 \pm 0.0008$	$0.0281 \pm 0.0006$

Assuming  $r_{CH} = 1.084 \pm 0.06$  Å.

shown in Table 7. Slight difference between calculated and observed  $J_{CH}$  for *para*-methine carbon will probably originate from the fact that rotational diffusion model can provide only approximate description of overall rotation of 2, 6-dichlorotoluene molecule. The set of dynamics parameters obtained from experimental data measured at two different fields are remarkably consistent despite the possible presence of many sources of experimental error such as pulse imperfection, relaxation during the preparation period of initial state of each magnetization mode, etc. We have also obtained *ca.* 1.73 for  $\tau_{int}^{(1)}/\tau_{int}^{(2)}$ , which may be interpreted as indicating that methyl group undergoes both three-fold and six-fold jumps at 25 °C.

**Acknowledgment.** The authors gratefully acknowledge the financial support they received from the SNU-Daewoo Research Fund during the fiscal year of 1995-1996.

## References

- Versmold, H. J. *Chem. Phys.* **1980**, *73*, 5310.
- Chung, D. S.; Kim, B. S.; Lee, J. W.; Shin, K. J. *Chem. Phys. Lett.* **1982**, *93*, 499.
- Wallach, D. J. *Chem. Phys.* **1967**, *47*, 5258.
- Abragam, A., 1961, *Principles of Nuclear Magnetism* (Oxford, London).
- Hubbard, P. S. *Phys. Rev.* **1963**, *131*, 1155.
- Bovey, F. A.; Jelinski, L.; Mirau, P. A. 1988, *Nuclear Magnetic Resonance Spectroscopy* (Academic, London).
- Vold, R. L.; Vold, R. R. *Prog. In NMR Spectrosc.* **1978**, *12*, 76.
- Werbelow, L. G.; Grant, D. M. *Adv. Magn. Reson.* **1977**, *9*, 189.
- Canet, D. *Prog. In NMR Spectrosc.* **1989**, *12*, 237.
- Lee, J. W.; Lim, M. H.; Rho, J-R. *Bull. Korean Chem. Soc.* **1991**, *12*, 47.
- Hubbard, P. S. *J. Chem. Phys.* **1969**, *51*, 1647.
- Haslinger, E.; Lynden-Bell, R. M. *J. Magn. Reson.* **1978**, *31*, 33.
- Matson, G. B. *J. Chem. Phys.* **1976**, *65*, 4147.
- Bull, T. E. *J. Chem. Phys.* **1990**, *93*, 6824.
- Konrat, R.; Sterk, H. *J. Phys. Chem.* **1990**, *94*, 1291.
- Zheng, Z.; Mayne, C. L.; Grant, D. M. *J. Magn. Reson. Ser. A.* **1993**, *103*, 268.
- Werbelow, L. G.; Grant, D. M. *J. Chem. Phys.* **1975**, *63*, 544.
- Kontaxis, G.; Muller, N.; Sterk, H. *J. Magn. Reson.* **1991**, *92*, 332.
- Grant, D. M.; Mayne, C. L.; Liu, F.; and Xiang, T. X. *Chem. Rev.* **1991**, *91*, 1591.
- Rho, J-R. *Ph. D. Thesis*, S. N. U. 1994 "A Study on Spin Dynamics in an  $AX_3$  Spin System".
- Konigsberger, E.; Sterk, H. *J. Chem. Phys.* **1985**, *83*, 2723.
- VNMR Software, User Programming Manual* (Varian Associates, 1994).
- Bevington, P. R. 1969, *Data Reduction and Error Analysis for the Physical Sciences* (McGraw-Hill).
- Press, W. H.; Flannery, B. P.; Teukolsky, S. A.; Vetterling, W. T. 1986, *Numerical Recipes-The Art of Scientific Computing* (Cambridge University).
- Werbelow, L. G.; Grant, D. M. *J. Chem. Phys.* **1975**, *63*, 4742.
- $\tau_D$  is invariant with respect to interchange of  $D_x$  and  $D_y$ , whence from the spectral density data alone one cannot tell which is larger. However, from geometrical consideration we assumed  $D_x > D_y$ .

## Appendix

The ensemble average of interest is

$$\langle \exp(im\gamma_0) \exp(-im'\gamma(t)) \rangle = \iint p(\gamma_0) p(\gamma, t | \gamma_0, 0) \exp(im\gamma_0) \exp(-im'\gamma) d\gamma d\gamma \quad [A1]$$

where  $\gamma$  is the rotation angle about a fixed internal axis and  $p(\gamma_0)$  is the probability that we find the internal rotation angle to be  $\gamma_0$  at time 0, and  $p(\gamma, t | \gamma_0, 0)$  is the conditional probability that the rotation angle is found to be  $\gamma$  at time  $t$  when it was known to be  $\gamma_0$  at time zero. This ensemble average can be evaluated on the basis of various molecular models:

(1) internal rotational diffusional model

If the reorientation of methyl group is described by rotational diffusion equation, then the conditional probability is shown to be given by

$$p(\gamma, t | \gamma_0, 0) = \sum_n (2\pi)^{-1} \exp(-in\gamma_0) \exp(in\gamma) \exp(-D_1 n^2 t) \quad [A2]$$

with *a priori* probability  $p(\gamma_0)$  being assumed constant so that

$$p(\gamma_0) = (2\pi)^{-1}. \quad [A3]$$

By making use of Eqs. [A2] and [A3] we obtain the expression

$$\langle \exp(im\gamma_0) \exp(-im'\gamma(t)) \rangle = \exp(-D_1 m^2 t) \delta_{m,m'} \quad [A4]$$

(2) 3-site jump model

If the reorientation consists of jumps among three equivalent sites,  $\gamma=0, 2\pi/3, 4\pi/3$ , then the ensemble average is

$$\langle \exp(im\gamma_0) \exp(-im'\gamma(t)) \rangle = \sum_{\gamma_0} \sum_{\gamma} p(\gamma_0) p(\gamma, t | \gamma_0, 0) \exp(im\gamma_0) \exp(-im'\gamma) \quad [A5]$$

The conditional probabilities are found by solving the linear differential equations for the fractional population at each site. If the fractional populations are denoted by  $[0], [2\pi/3], [4\pi/3]$ , these equations may be written as

$$\frac{d}{dt} \begin{pmatrix} [0] \\ [2\pi/3] \\ [4\pi/3] \end{pmatrix} = \frac{1}{\tau} \begin{pmatrix} -2 & 1 & 1 \\ 1 & -2 & 1 \\ 1 & 1 & -2 \end{pmatrix} \begin{pmatrix} [0] \\ [2\pi/3] \\ [4\pi/3] \end{pmatrix} \quad [A6]$$

where 1/τ is the rate of jump from one site to another. Combined with the conservation equation [0] + [2π/3] + [4π/3] = 1 and the initial condition [0] = 1, and assuming that a priori probabilities are all equal, that is,

$$p(\gamma_0) = 1/3. \quad [A7]$$

we find the conditional probabilities as

$$\begin{aligned} p(0, t | 0, 0) &= \frac{1}{3} + \frac{2}{3} \exp(-3t/\tau) \\ p(2\pi/3, t | 0, 0) &= \frac{1}{3} - \frac{1}{3} \exp(-3t/\tau) \\ p(4\pi/3, t | 0, 0) &= \frac{1}{3} - \frac{1}{3} \exp(-3t/\tau) \end{aligned} \quad [A8]$$

Substitution of this equation into Eq. [A5] leads to

$$\begin{aligned} \langle \exp(im\gamma_0) \exp(-im\gamma(t)) \rangle &= \delta_{m,0} \delta_{m',0} + \exp(-3t/\tau) \\ &(\delta_{m,m'} - \delta_{m',0} \delta_{m,0} + \delta_{m,m'+3} \delta_{m,m'-3}) \end{aligned} \quad [A9]$$

### (3) 6-site jump model (I)

If we consider that the reorientation consists of jumps between only nearest sites among the 6-equivalent sites, γ = 0, π/3, 2π/3, 3π/3, 4π/3, 5π/3, the conditional probabilities can be obtained by the procedure similar to that applied to 3-site jump model. The master equation may be written in this case

$$\frac{d}{dt} \begin{pmatrix} [0] \\ [\pi/3] \\ [2\pi/3] \\ [3\pi/3] \\ [4\pi/3] \\ [5\pi/3] \end{pmatrix} = \frac{1}{\tau} \begin{pmatrix} -2 & 1 & 0 & 0 & 0 & 1 \\ 1 & -2 & 1 & 0 & 0 & 0 \\ 0 & 1 & -2 & 1 & 0 & 0 \\ 0 & 0 & 1 & -2 & 1 & 0 \\ 0 & 0 & 0 & 1 & -2 & 1 \\ 1 & 0 & 0 & 0 & 1 & -2 \end{pmatrix} \begin{pmatrix} [0] \\ [\pi/3] \\ [2\pi/3] \\ [3\pi/3] \\ [4\pi/3] \\ [5\pi/3] \end{pmatrix} \quad [A10]$$

With the assumption that a priori probabilities are equal to 1/6, solving this system gives the following conditional probabilities:

$$\begin{aligned} p(0, t | 0, 0) &= \frac{1}{6} \{ \exp(-4t/\tau) + 2\exp(-3t/\tau) + 2\exp(-t/\tau) + 1 \} \\ p(\pi/3, t | 0, 0) &= -\frac{1}{6} \{ \exp(-4t/\tau) + \exp(-3t/\tau) - \exp(-t/\tau) - 1 \} \\ &= p(5\pi/3, t | 0, 0) \\ p(2\pi/3, t | 0, 0) &= \frac{1}{6} \{ \exp(-4t/\tau) - \exp(-3t/\tau) - \exp(-t/\tau) - 1 \} \end{aligned}$$

$$= p(4\pi/3, t | 0, 0)$$

$$\begin{aligned} p(3\pi/3, t | 0, 0) &= \frac{1}{6} \{ -\exp(-4t/\tau) + 2\exp(-3t/\tau) \\ &- 2\exp(-t/\tau) + 1 \} \end{aligned} \quad [A11]$$

From these conditional probability, we find the ensemble averages of interest:

$$\langle \exp(i\gamma_0) \exp(-i\gamma(t)) \rangle = \exp(-t/\tau) \quad [A12]$$

$$\langle \exp(2i\gamma_0) \exp(-2i\gamma(t)) \rangle = \exp(-3t/\tau) \quad [A13]$$

### (4) 6-site jump model (II)

Here we assume that the jumping occurs not only between the nearest sites but also between next to the nearest neighboring sites. Then the differential equation for this model is slightly different from the previous one as shown in Eq. [A14]:

$$\frac{d}{dt} \begin{pmatrix} [0] \\ [\pi/3] \\ [2\pi/3] \\ [3\pi/3] \\ [4\pi/3] \\ [5\pi/3] \end{pmatrix} = \frac{1}{\tau} \begin{pmatrix} -4 & 1 & 1 & 0 & 1 & 1 \\ 1 & -4 & 1 & 1 & 0 & 1 \\ 1 & 1 & -4 & 1 & 1 & 0 \\ 0 & 1 & 1 & -4 & 1 & 1 \\ 1 & 0 & 1 & 1 & -4 & 1 \\ 1 & 1 & 0 & 1 & 1 & -4 \end{pmatrix} \begin{pmatrix} [0] \\ [\pi/3] \\ [2\pi/3] \\ [3\pi/3] \\ [4\pi/3] \\ [5\pi/3] \end{pmatrix} \quad [A14]$$

The conditional probabilities for this model are found to be given as follows:

$$\begin{aligned} p(0, t | 0, 0) &= \frac{1}{6} \{ 2 \exp(-6t/\tau) + 3 \exp(-4t/\tau) + 1 \} \\ p(\pi/3, t | 0, 0) &= \frac{1}{6} \{ -\exp(-6t/\tau) + 1 \} \\ &= p(5\pi/3, t | 0, 0) \\ p(2\pi/3, t | 0, 0) &= \frac{1}{6} \{ -\exp(-6t/\tau) + 1 \} \\ &= p(4\pi/3, t | 0, 0) \\ p(3\pi/3, t | 0, 0) &= \frac{1}{6} \{ 2 \exp(-6t/\tau) + 3 \exp(-4t/\tau) + 1 \} \end{aligned}$$

Thus we can obtain in this case the following expressions:

$$\langle \exp(i\gamma_0) \exp(-i\gamma(t)) \rangle = \exp(-4t/\tau) \quad [A16]$$

$$\langle \exp(2i\gamma_0) \exp(-2i\gamma(t)) \rangle = \exp(-6t/\tau) \quad [A17]$$